A dielectric study of the domain freezing in KD_2AsO_4

A dielectric study of the domain freezing in KD$_2$AsO$_4$

M Fally†, P Kubinec†§, A Fuith†, H Warhanek† and C Filipič‡

† Universität Wien, Institut für Experimentalphysik, Strudlhofgasse 4, A-1090 Wien, Austria
‡ University of Ljubljana, Jožef Stefan Institute, 61111 Ljubljana, Slovenia

Abstract. The temperature- and frequency-dependent dielectric susceptibility of KD$_2$AsO$_4$ was studied in the ferroelectric phase. A dispersion which is related to the dipole reversal was found in the high-frequency range (10^7 Hz). The dispersion is described by a Gaussian distribution of relaxation times [1] which show Vogel–Fulcher temperature dependences. The high value of the dielectric constant below the phase transition is related to the mobility of the domain walls. This mobility steeply decreases near the freezing temperature T_f and therefore a sudden decrease in the susceptibility takes place. A non-linear superposition of the piezoelectric resonance and the relaxational dispersion was observed.

1. Introduction

KD$_2$AsO$_4$ is isostructural to KH$_2$PO$_4$ and undergoes a para–ferroelectric phase transition at $T_c = 162.5$ K. The dielectric properties of members of the KDP family in this ferroelectric phase were studied from various points of view [1, 5] and are somewhat different from what one would expect from Landau theory: the temperature dependence of the dielectric constant, ϵ_c, shows a plateau region from T_c down to a temperature $T_f = 143$ K, where a steep decrease takes place. We define T_f as the temperature where $\partial^2\epsilon_0/\partial T^2 = 0$ (ϵ_0: static permittivity). For KH$_2$PO$_4$ this behaviour was explained by the temperature dependence of the mobility of the domain walls and is called 'domain freezing' [6].

The frequency dependence of the dielectric susceptibility displays two dispersions: one is of resonance type due to the piezoelectric stimulation (100 kHz region) and a second one, at high frequencies (10 MHz region), is of relaxational type. The latter one shows the following temperature dependence: at T_c the maximum of the dielectric loss $\epsilon''(\omega)$ takes place at approximately $2\pi \times 10^7$ Hz. On lowering the temperature the maximum shifts towards lower frequencies until the relaxation time goes to infinity at $T_0 < T_f$, i.e. the relaxation vanishes.

In [1] Kuramoto has suggested a phenomenological *ansatz* for the description of the complex dielectric constant. He assumes a non-linear behaviour of the contributions of the two dispersions in the vicinity of the freezing temperature T_f and multiplies their contributions. He also assumes a Gaussian distribution of relaxation times [7] with a Vogel–Fulcher temperature dependence of each relaxation time. In this work we present the dielectric susceptibility of KD$_2$AsO$_4$ and apply the mentioned approach of Kuramoto [1].

§ Permanent address: Technical University of Transport and Communication, Department of Physics, 01026 Žilina, Slovakia.

2. Experimental details

The crystals were grown by a temperature gradient method from a deuterated aqueous solution with an enhanced pH value of approximately pH $\approx$ 6.
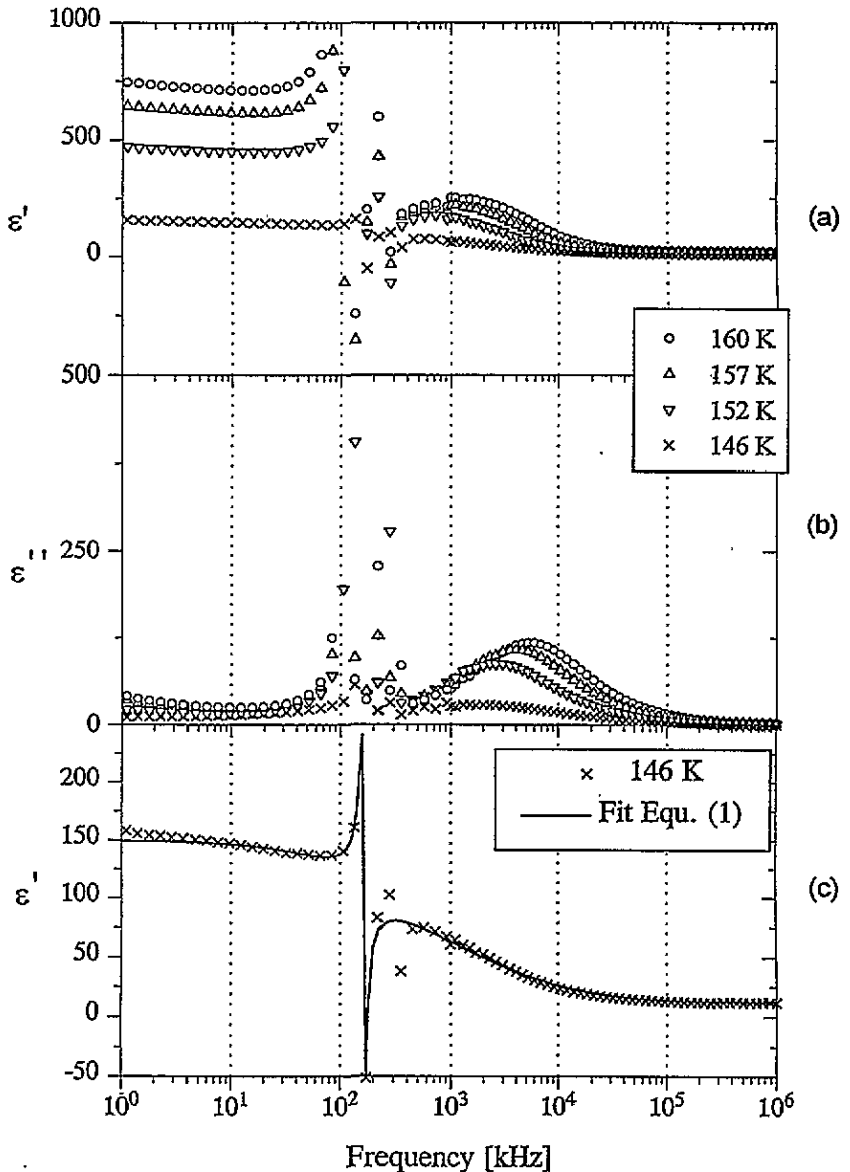

Figure 1. Frequency dependence of (a) ϵ' and (b) ϵ'' at various temperatures in the ferroelectric phase. (c) Frequency dependence of ϵ' and ϵ'' at $T = 146$ K. The solid line displays a least-squares fit to equation (1).

The sample was cut out of the pyramidal sector of the crystal grown and is lossy in the sense that the crystal contains chemical impurities. This is the case because the arsenates have to be grown in a more alkaline solution, which means that one has to add a large
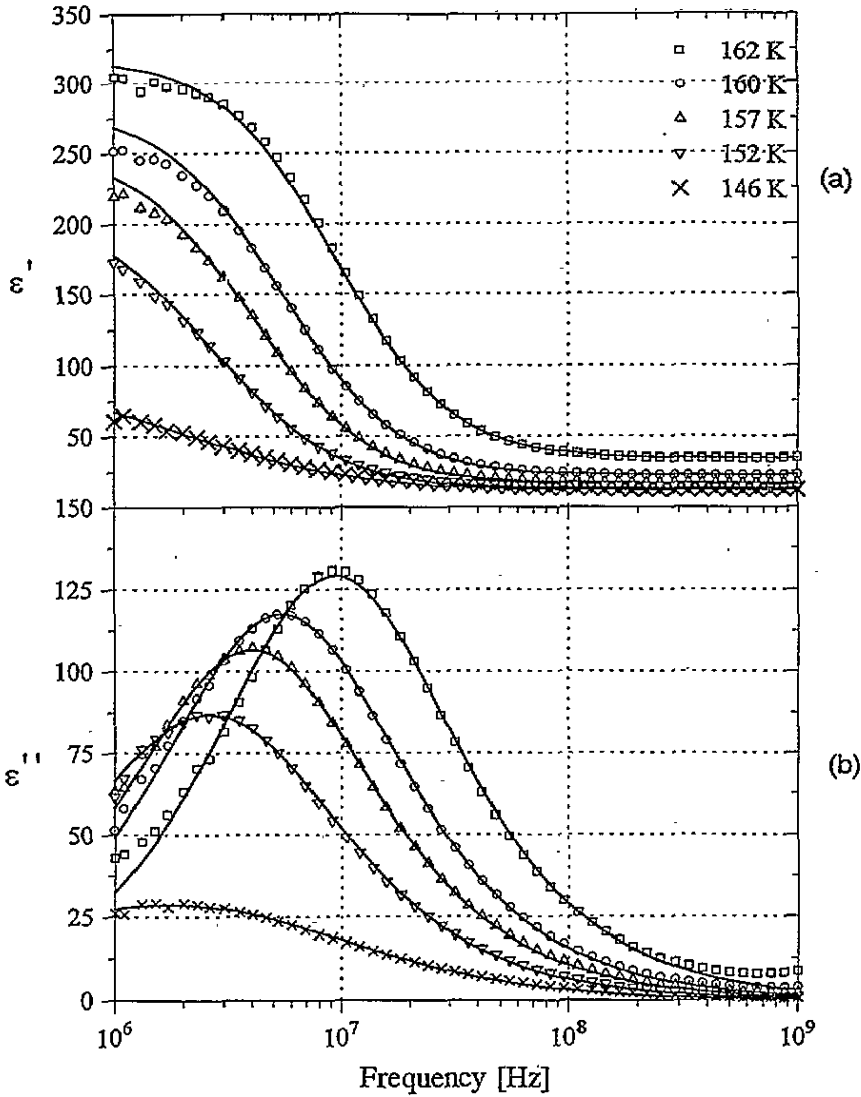
Figure 2. Relaxational part of the dielectric susceptiblity (a) ϵ' and (b) ϵ'' at high frequencies. Solid lines indicate least-squares fits to equation (9) with the parameters C and D of figure 6.

amount of KOD [9]. Because of this fact the dielectric loss increases to quite high values above room temperature (see figure 3(a)) [1].

The measurements have been performed on a circular c-platelet (parallel to the ferroelectric axis) with dimensions 5.9 mm in diameter and 1.54 mm in thickness with electrodes of evaporated silver or silver paste. Comparing the results for both types of electrode no differences were observable. The complex dielectric constant $\epsilon^* = \epsilon' - i\epsilon''$ was measured using an HP 4284A impedance analyser from 20 Hz to 1 MHz, an HP 4192A LF from 1 kHz to 13 MHz and an HP 4191A RF from 1 MHz to 1 GHz. The static measurement was made by a Keithley 617 Electrometer. The temperature was stabilized by an Oxford Instruments continuous flow cryostat or a closed cycle CTI-Cryogenics
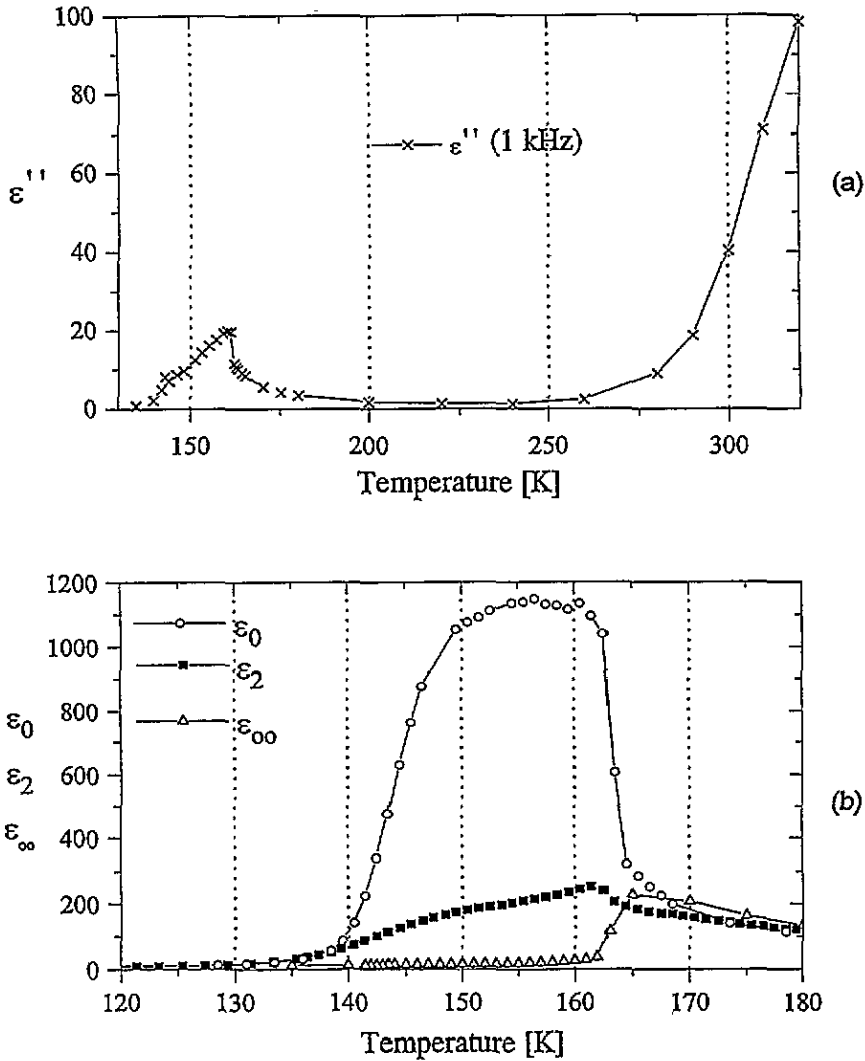
Figure 3. (a) Temperature dependence of the dielectric loss up to room temperature at low frequencies. (b) Temperature dependence of the dielectric permittivity of the free crystal ϵ_0, the clamped crystal ϵ_2 and the high-frequency limit ϵ_∞.

Cryodyne 22 respectively.

For the measurements with various applied DC fields we used a General Radio Bridge. In this case the shape of the sample was rectangular with dimensions $4.2 \times 6.8 \times 0.34$ mm^3. The AC voltage was below 0.7 V in all cases ($E = 4.5$ V cm^{-1} for the circular sample).

3. Results

In figures 1 and 2 the dielectric constant versus frequency is shown at various temperatures. Figure 2 highlights the relaxational part of the dielectric constant. Figure 3(b) gives the temperature dependence of the susceptibility as measured at 'special' frequencies, namely ϵ_0 ($f = 0$) by a static measurement, ϵ_∞ at 1 GHz (high-frequency limit) and ϵ_2 (clamped
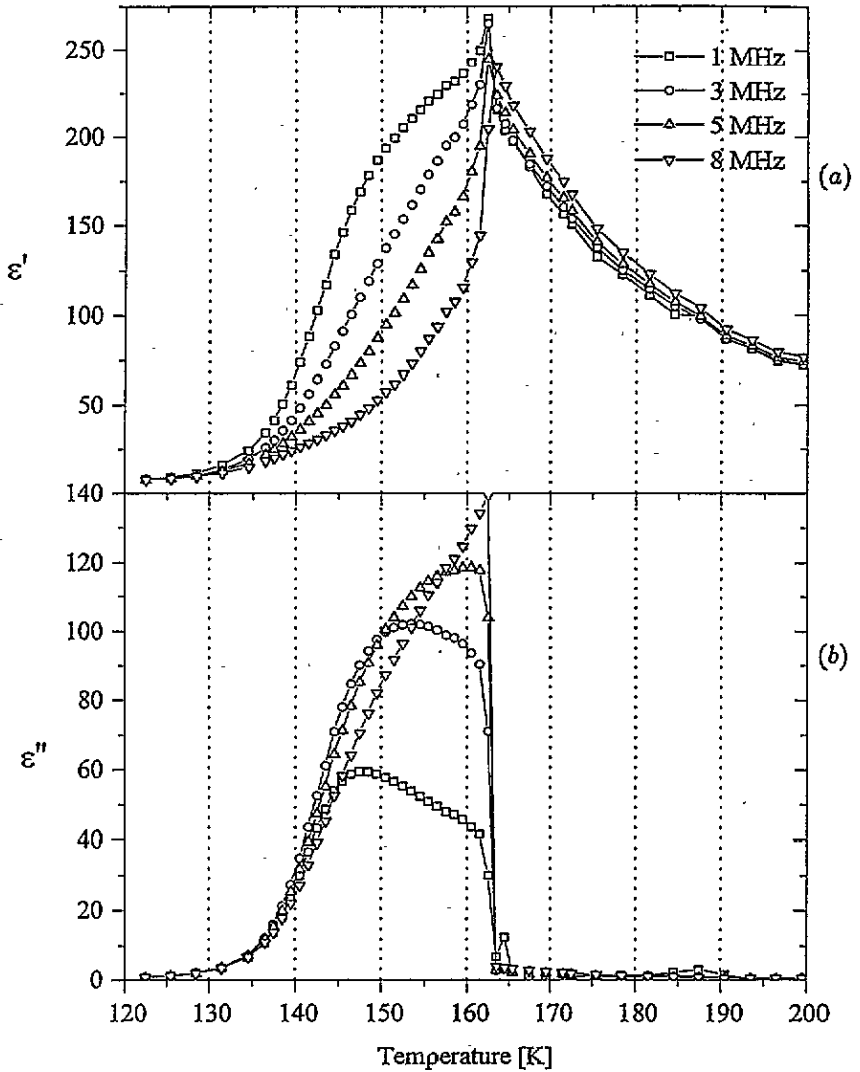
Figure 4. Temperature dependences of the dielectric constant at various frequencies: (a) ϵ' and (b) ϵ''.

crystal) at $f \approx 1$ MHz. The temperature dependences of ϵ^* at various frequencies are represented in figure 4.

The total dielectric constant in the presence of the piezoelectric resonance and the relaxational dispersion can be written as [1]

$$\epsilon^*(\omega, T) = [\epsilon_0(T) - \epsilon_2(T)]\epsilon_{res}^*(\omega, T)\epsilon_{rel}^*(\omega, T) + [\epsilon_2(T) - \epsilon_\infty(T)]\epsilon_{rel}^*(\omega, T) + \epsilon_\infty(T).$$

$$(1)$$

This implies that the behaviour of the dielectric constant cannot be described by a simple linear superposition of the two contributions.
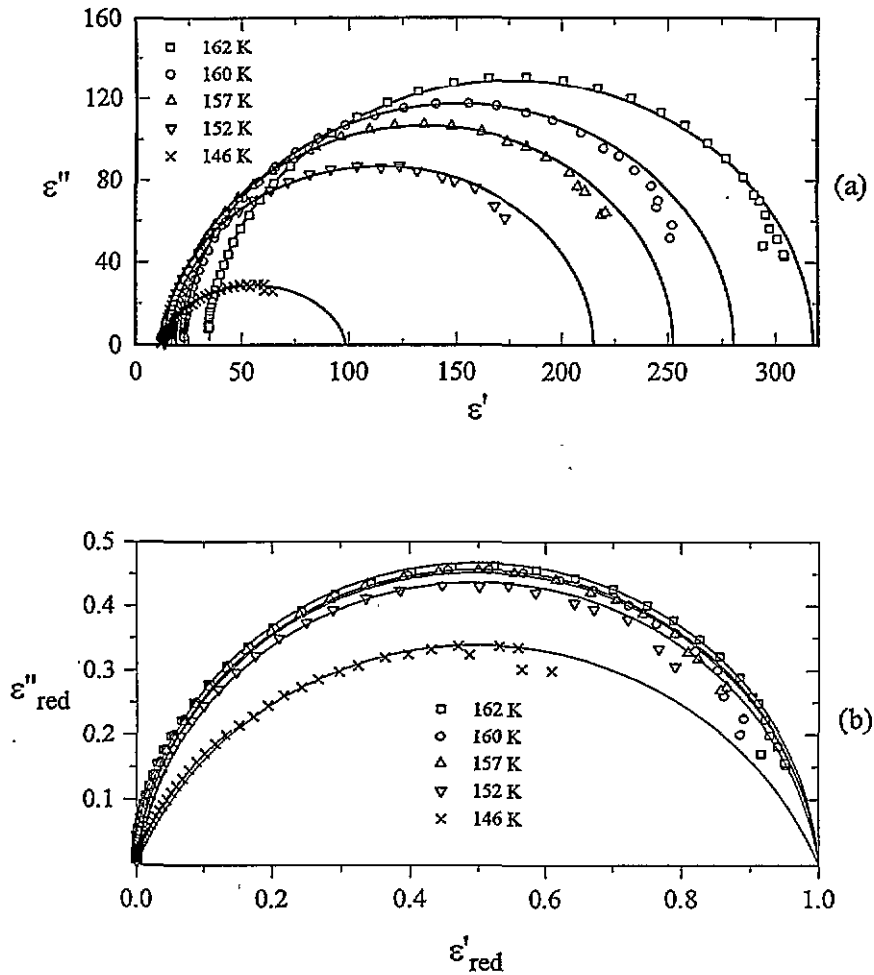
Figure 5. Argand diagrams of the same regime as in figure 2. (a) Fully temperature-dependent Cole–Cole plots. Solid lines are fits to (9) with parameters of figure 6. (b) Reduced Cole–Cole plots. Solid lines in (b) are fits to (9).

The resonance part here is

$$\epsilon_{res}^{*}(\omega, T) = \frac{\omega_0^2(T)}{\omega_0^2(T) - \omega^2 + i\gamma(T)\omega} \qquad (2)$$

where ω_0 denotes the resonance frequency and γ the damping constant.

The relaxational part involves a distribution $g(\tau, T)$ of relaxation times τ [8],

$$\epsilon_{rel}^{*}(\omega, T) = \int_0^\infty \frac{g(\tau, T)}{1 + i\omega\tau} \frac{d\tau}{\tau} \qquad (3)$$

which obey a Vogel–Fulcher temperature dependence

$$\tau(T) = \tau_0 \exp\left\{\frac{E}{T - T_0}\right\}. \qquad (4)$$

The distribution $f(E)$ for the activation energies E entering the Vogel–Fulcher law is chosen as Gaussian, so that with $g(\tau, T) = f(E)(T - T_0)$

$$f(E) = \frac{1}{\sqrt{2\pi}\sigma} \exp\left\{\frac{-(E - E_0)^2}{2\sigma^2}\right\} \tag{5}$$

$$g(\tau, T) = \frac{T - T_0}{\sqrt{2\pi}\sigma} \exp\left\{\frac{-[(T - T_0)(\ln\tau - \ln\tau_0) - E_0]^2}{2\sigma^2}\right\}. \tag{6}$$

σ is the variance of the distribution and T_0 is the (Vogel–Fulcher) temperature at which the relaxation time approaches infinity.

4. Discussion

4.1. Relaxation

As long as $\omega_{\max}(\epsilon'') \gg \omega_0$ one can treat the two contributions to ϵ^* in equation (1) separately. Then for the high-frequency region one can write:

$$\epsilon^*(\omega, T) - \epsilon_\infty(T) \simeq [\epsilon_2(T) - \epsilon_\infty(T)] \epsilon^*_{\text{rel}}(\omega, T). \tag{7}$$

With the substitution $x = \ln\tau$ and the convenient abbreviations

$$B(T) = [\epsilon_2(T) - \epsilon_\infty(T)]\frac{T - T_0}{\sqrt{2\pi}\sigma}$$

$$C(T) = \frac{1}{\sqrt{2}\sigma}(T - T_0) \tag{8}$$

$$D(T) = \frac{(T - T_0)\ln\tau_0 + E_0}{\sqrt{2}\sigma}$$

and using equation (3) one arrives at

$$\epsilon^*_{\text{rel}}(\omega, T) - \epsilon_\infty(T) = B(T) \int_{-\infty}^{\infty} \frac{\exp\left\{-[C(T)x - D(T)]^2\right\}}{1 + i\omega\,e^x}\,dx. \tag{9}$$

Figure 5 shows Cole–Cole plots (Argand diagrams) for frequencies 1 MHz–1 GHz and at several temperatures $T_0 < T < T_c$. With decreasing temperature the relaxation remains symmetric but becomes broader as can be seen more clearly by drawing a reduced Cole–Cole plot (figure 5(b)). $\epsilon_\infty(T)$ is taken at 1 GHz and $\epsilon_2(T)$ is calculated by making use of the Kramers–Krönig relations which yield

$$\int_0^{\infty} \epsilon''(\omega)\,d[\ln\omega] = \frac{\pi}{2}(\epsilon_2 - \epsilon_\infty). \tag{10}$$

The integral can be evaluated from the experimental data quite accurately by assuming $\epsilon''(\omega)$ to be symmetric and to vanish for frequencies larger than $\omega > 2\pi \times 10^9$ Hz.

Least-squares fits for the relaxation part in $\epsilon''(\omega)$ (solid lines in figure 2 and figure 5(a)) were performed in the temperature region from 162 K to 141 K using equation (9). Figure 6 shows the temperature dependences of the parameters $C(T)$, $D(T)$ from equation (9).

Using equation (1) and fitting $\epsilon''(\omega)$ for the whole frequency range between 10 kHz and 1 GHz, it is shown that the approach of Kuramoto [1] fits the experimental data quite well (solid line in figure 1(c)). We did this procedure only for the temperature $T = 146$ K because the information which we get out additionally (e.g. parameters $\epsilon_0, \gamma, \omega_0$) is not really interesting with respect to the domain freezing problem.

By working out linear regression for the parameters $C(T)$ and $D(T)$ one can determine values for τ_0, T_0, E_0 and σ. This leads to $\tau_0 = (2.78 \pm 0.78) \times 10^{-8}$ s, $T_0 = 139.6 \pm 0.22$ K,
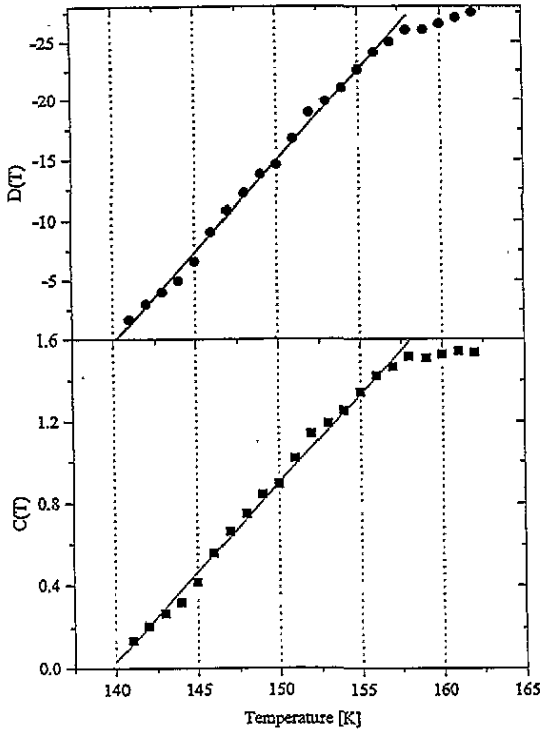
Figure 6. Temperature dependence of the fitting parameters C and D from equation (9).

$E_0 = 8.9 \pm 3.15$ K and $\sigma = 8.2 \pm 0.16$ K. Note that $\sigma \approx E_0$ which may be an indication of a wide distribution of domain sizes.

4.2. Resonance

The investigated crystal shows at least two strong mechanical resonances due to piezoelectric stimulation. The resonance frequencies depend on the size and the shape of the sample. Due to symmetry there is a piezodistortive (bilinear) coupling between the polarization P_3 and the strain e_6

$$P_3 = d_{36}S_6 = d_{36}C_{66}e_6 \tag{11}$$

with P, d, S, C, e referring to the polarization, the piezoelectric constant, the stress, the elastic constant and the strain, respectively. We investigated the temperature dependence of the lowest resonance frequency because from that one can easily calculate the elastic shear constant C_{66} [9]. Figure 7 shows the temperature dependence of the elastic constant C_{66} and the damping constant $\gamma(T)$. Note that the maximal damping does not occur at the phase transition temperature but at the freezing temperature.

4.3. DC bias

We also performed measurements at different DC bias fields of $E = 0$ kV cm^{-1}, 5.6 kV cm^{-1}, 8 kV cm^{-1} and 12 kV cm^{-1} at the frequency $f = 1$ kHz using the high-resolution General Radio Bridge. No influence on the dielectric permittivity at such high fields could be
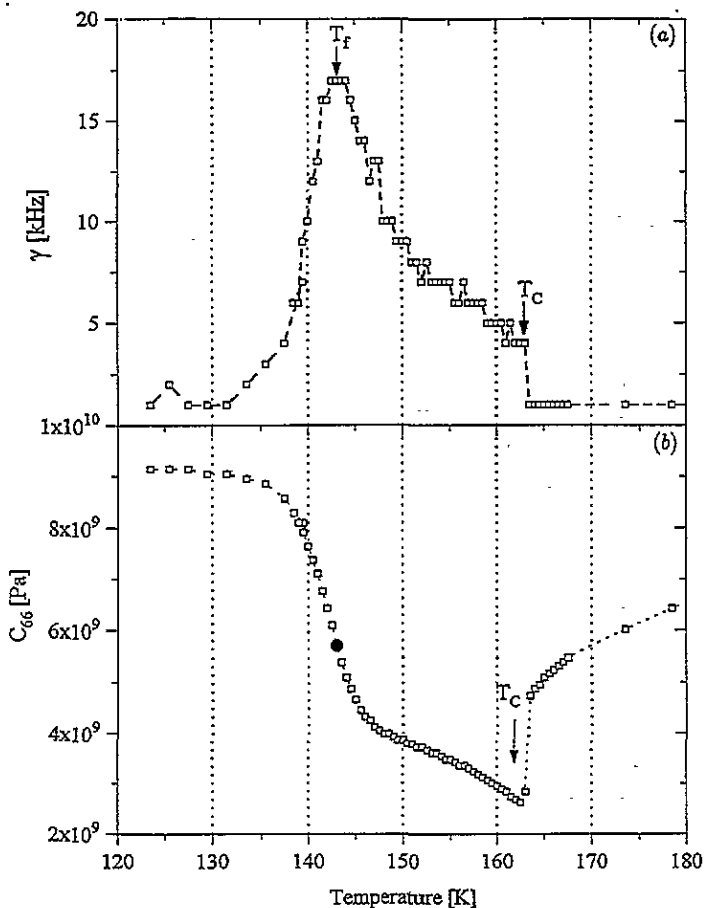
Figure 7. (a) Temperature dependence of the damping constant $= \gamma(T)$ at the first piezoelectric resonance. (b) Temperature dependence of the elastic constant $C_{66}(T)$ calculated from the first resonance frequency.

observed. This is in contrast to the corresponding phosphates, where at 8 kV cm^{-1} one can see a strong decrease of ϵ', which indicates monodomainization [9].

5. Conclusion

We have investigated KD_2AsO_4 in the ferroelectric phase by means of dielectric measurements over a wide frequency region. Similiar features as in the phosphates occur, namely a resonance dispersion at low frequencies (depending on the size of the sample and the temperature) and a relaxational dispersion in the high-frequency region (≈ 10 MHz). The relaxation is due to the reversal of the dipoles in the AC field, i.e. the domain walls can move and the reorientation of the corresponding dipoles enlarges the susceptibility. So the real part of the dielectric constant below the phase transition remains at high values over a temperature range of approximately 20 K. When approaching a certain temperature T_f the dipoles are no longer easily removeable and consequently the mobility of the domain walls vanishes, leading to an abrupt decrease of the dielectric constant.

It should be mentioned that the effect of the domain freezing could be influenced by the defect structure of the sample very much [2, 10, 11]. Until now only mobile point defects [10] were taken into account in the theoretical treatment. Bornarel [2] remarked that dislocations play an important role for the mobility of domain walls. As the arsenates have a rather high photoelectric absorption, characterization by means of x-ray topography is not as simple as for the phosphates. A characterization of the defect structure of the samples is in progress.

Acknowledgments

References

[1] Kuramoto K 1987 *J. Phys. Soc. Japan* **56** 1859
[2] Bornarel J 1972 *J. Appl. Phys.* **43** 845
[3] Kamysheva L and Drozhdin S 1987 *Ferroelectrics* **71** 281
[4] Chabin M and Giletta F 1977 *Ferroelectrics* **15** 149
[5] Barkla H M and Finlayson D M 1953 *Phil. Mag.* **44** 109
[6] Fedosov V and Sidorkin A 1977 *Sov. Phys.–Solid State* **19** 1359
[7] Hill R and Ichiki S 1962 *Phys. Rev.* **128** 1140
[8] Courtens E 1984 *Phys. Rev. Lett.* **52** 69
[9] Nakamura E and Kuramoto K 1988 *J. Phys. Soc. Japan* **57** 2182
[10] Sidorkin A and Fedosov V 1977 *Sov. Phys.–Solid State* **19** 1024
[11] Nakamura E 1992 *Ferroelectrics* **135** 237